VIII International Conference on Computational Methods for Coupled Problems in Science and Engineering
COUPLED PROBLEMS 2019
E. Oñate, M. Papadrakakis and B. Schrefler (Eds)

AEROELASTIC-STRUCTURAL COUPLING IN ANTENNA PROTOTYPE FOR WINDY OPEN-SPACE

G. IUSO[*], G. VIRONE[†], G. CAFIERO[*], E. BONISOLI[*], D. LISITANO[*], S. VENTURINI[*]

[*] Politecnico di Torino, Department of Mechanical and Aerospace Engineering
Corso Duca degli Abruzzi, 24 – 10129 Torino, Italy
e-mail: {name.surname}@polito.it

[†] Consiglio Nazionale delle Ricerche, Istituto di Elettronica ed Ingegneria dell'Informazione e delle Telecomunicazioni, Corso Duca degli Abruzzi, 24 – 10129 Torino, Italy
e-mail: giuseppe.virone@ieiit.cnr.it

Key words: Wind tunnel, Experimental fluid-structure interaction, Coincident eigenvalues, High-density modal content.

Abstract. The interaction between wind and an antenna prototype for the low-frequency radio telescope of the Square Kilometer Array (SKA) is experimentally tested in the wind tunnel of the Politecnico di Torino. The tests aim to predict the antenna behaviour during working conditions, i.e. mounted by means of five contact points to a metal grid on sandy ground in the Australian desert.

The wind tunnel is characterised by a circular test section having a diameter equal to 3 m and a length equal to 5 m. The height and the distance between the lateral legs of the antenna are equal respectively to 2.2 m and 1.5 m. The tests were performed at increasing wind speed up to 110 km/h. The system under analysis is an aluminium antenna composed by four parts arranged in axial symmetry and each one made of fifteen rods and small plates/wire elements.

A numerical parametric model of the system is developed to numerically study the dynamic behaviour of the antenna in the frequency range of interest. The model is able to handle very high modal density and closed spaced modes in multiplicity of four because of the symmetric structure as well as the different shapes of the elements forming the antenna. The wind tunnel results emphasise the fluid-structure coupling of aerodynamics modes and the critical aspects of the boundary conditions for a good prediction of the oscillations amplitudes.

1 INTRODUCTION

The Square Kilometer Array (SKA) represents the near future of radio astronomy [1]. Both the low- (50-350 MHz) and mid-frequency (500-1500 MHz) instruments (to be deployed in the first and second phase of the SKA construction) will be implemented as Aperture Arrays having hundreds of thousands digitally-beamformed antenna elements.

The current baseline for the array element of the low–frequency instrument is a dual-polarized log-periodic configuration [2,4] with 16 elements, a total height from the ground of

about 2.1 m and a base width of 1.6 m, which is better described in the following. Besides the electromagnetic tests campaigns in outdoor environment [5,6] and semi-anechoic chamber, the prototype requires several qualifications for environmental parameters, as the wind-loading effect. The antenna should be able to survive a wind speed of about 100 km/h and to operate without significant deformations up to 60 km/h.

Aerodynamically speaking an antenna can be considered as a bluff boy when an interaction with an air flow takes place. The flow separation usually occurs around a body immersed in a stream. The region of detached flow (wake) is highly unsteady and contains a great variety of flow structures more or less organized and characterized by typical temporal and space scales ranging over different order of magnitude. The unsteady separated flow plays a key role in the aerodynamic excitation of the immersed body which as a consequence is characterized by a time dependent pressure distribution around the body that in turn originates time dependent forces. Particularly interesting is the shedding phenomenon characterized by the release of organized vortices that induce unsteady forces in the body [7]. The unsteadiness of the separated flow is the origin of different forms of aeroelastic instabilities such as the galloping [8], the buffeting and the flutter of the structure. The turbulence intrinsically present in the atmospheric wind influences the loads acting on a structure. Many studies are present in the literature focused on the investigation of wind-structures interaction that involves different engineering fields. Wind-bluff bodies interactions including buildings, bridges, towers, cables, are of great interest for civil engineering applications. The interaction related to antennas and the atmospheric wind is also largely analysed as shown by many papers published on this subject such as [9,11].

The aims of this work are: a) to develop and validate a structural model of the system useful to forecast the effect of antenna design changes on the dynamic behaviour of the antenna, b) to identify and to analyse the effect of aeroelastic modes given by the fluid structure interaction and c) to correlates aeroelastic modes with the antenna components.

To reach these aims, standard experimental modal analysis (EMA) is performed on the system, coupled with signature acquisition under wind excitation. Experimental modal analysis is nowadays the most used technique to acquire the dynamic behaviour of components and systems [12]. Numerical simulations on components and systems are common use in industrial fields and very often they are used for improving the design phase. EMA and other dynamics test are used to validate the numerical models and to check the actual operating conditions. Usually model updating [13] is necessary to obtain realistic model and boundary conditions are critical for the operational working condition [14]. The investigation carried out in the wind tunnel complete the validation of the whole methodology.

2 ANTENNA PROTOTYPE: EXPERIMENTAL SET UP IN THE WIND TUNNEL AND NUMERICAL MODEL

The antenna prototype under analysis, shown in Figure 1 (a), is an axially symmetric structure in Aluminum constrained to a metal grid, manufactured by Sirio Antenne [5]. A planar tree-like module is circularly repeated four times each 90 degree. The module is made several beam elements. The main body is a boxed beam 2.1 m long, cross section 25x15 mm rectangular beam and 2 mm thick walls. Nine branches are attached on the biggest face of the

main beam, in alternation between left and right side. The branches are triangular paths, created with circular cross section, diameter $\phi = 5$ mm, their length is scaled from 0.7 m (low part) to 0.2 m (top part). The main body is supported with a bigger circular beam 0.8 m long, attached at 0.51 m of the main body and to the metal grid. The constraint with the metallic grid is a Teflon support Figure 1 (b), including two rigid kinematic hinges around the axis perpendicular to the main beam direction. This support is also linked to the main body with other two thinner circular beam, diameter $\phi = 5$ mm. Six triangular thin plates are attached to the main beam in the top part. Support beam branches and plates are placed alternatively on left and right side of the elementary structure.

The four modules are linked together with four Teflon constraint on the main beams, shown in Figure 1 (d), located at $0.45, 0.65, 1.22, 1.75$ m from the ground. The four main beams are constrained to the ground grid by means of translation constraint, shown in Figure 1 (c). The metallic grid is fixed to the ground in four points.

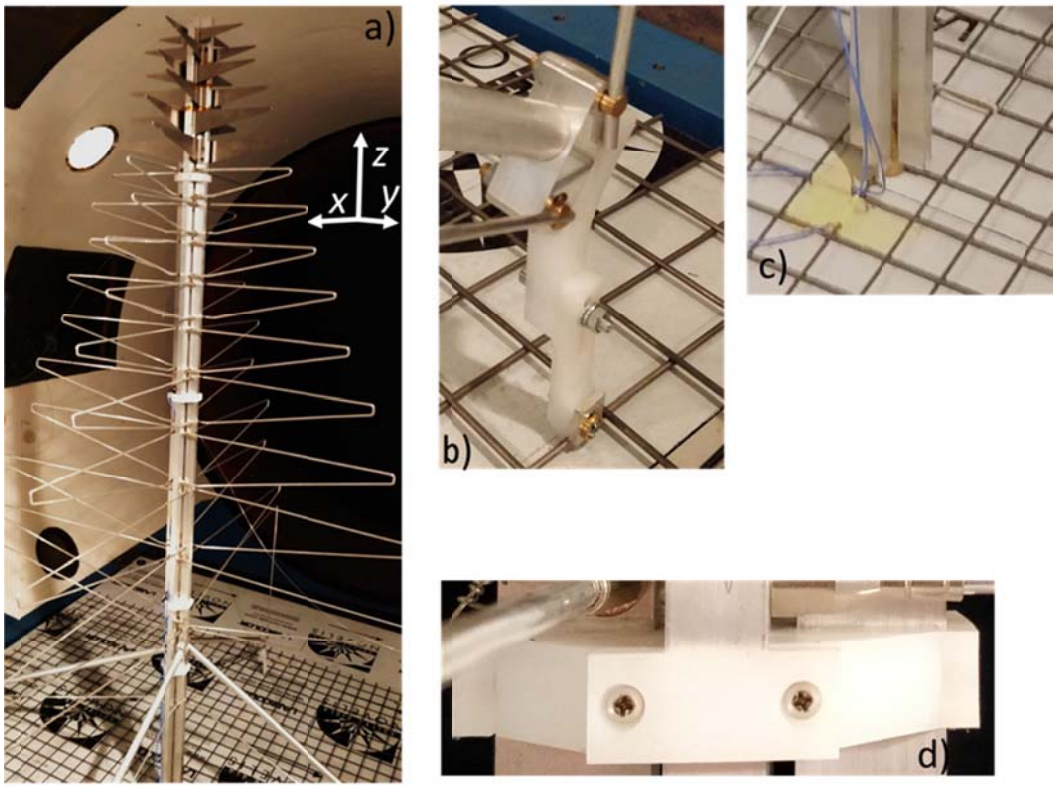

Figure 1: System under analysis: a) antenna, b) supports constraints c) central constraint and d) main beam constraint.

2.1 Experimental setup

The fluid structure interaction is experimentally investigated in subsonic wind tunnel of the Politecnico di Torino. The circuit of the wind tunnel is closed, the test section is circular characterized by a diameter of 3 m and a length of 5 m. The maximum speed available is

equal to 80 m/s. A flat plate was mounted in the test section simulating the ground of the real case. Moreover, a metal grid having the same geometric characteristics of the actual configuration was fixed to the plate through fixing points positioned on three peripheral sides simulating the same constrains conditions of the real case. In Figure 2 the antenna mounted in the test section is shown. The tests were performed at four different uniform wind speeds, without the simulation of the typical velocity distribution of the atmospheric boundary layer.

The accelerations are measured in the two points ($z_1 = 0.65\,\text{m}$ and $z_2 = 1.22\,\text{m}$), where accelerometers PCB 356A15 are located. The measurements were performed collecting data at the sampling frequency equal to 10240 Hz. LMS Scadas mobile and Test.Lab software were used to acquire and to post-process the time domain data.

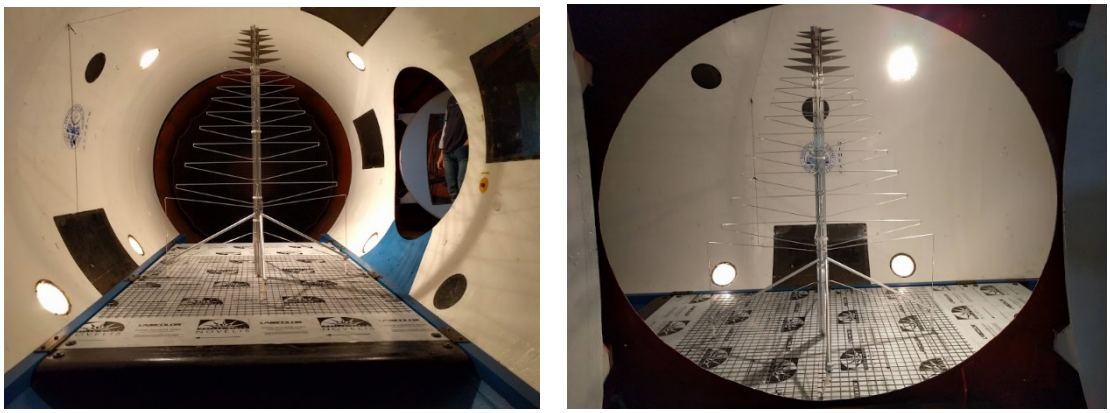

Figure 2: The antenna mounted in the test section of the wind tunnel.

The global behaviour of the antenna was monitored by means of two cameras mounted outside of the test section. The cameras were positioned so that the deformations in the vertical plane xz and in plane xy parallel to the wall were visible. Different tests were carried out with the goal of reducing the deformation of the antenna varying the constraints configuration of the antenna-grid fixing points.

Roving hammer test modal analysis is performed on the antenna structure in condition of wind off, to identify the first global structural modes of the system. LMS Scadas mobile and Test.Lab software were used to acquire data and to perform the EMA. Ten points are selected on the main beams of the structure, one each $0.3\,\text{m}$, and the two nodes on the second and third Teflon constraints, on which two triaxial accelerometers are located. The structure is excited in the ten points along the two directions perpendicular to the main beam, using an instrumented hammer PCB 086C03. The sample frequency is 4096 Hz, therefore the frequency response functions within 2048 Hz are measured with a frequency resolution of 0.125 Hz. Force exponential windows is applied to the input force signal and exponential windows is applied on the measured responses.

2.2 Numerical model

A finite element (FE) model is developed in LUPOS environment to perform numerical modal analysis of the structure, in condition of wind off. LUPOS is a parametric FE codes, developed in Politecnico di Torino [15], which is able to handle very well tri-dimensional

systems which can be schematised using mono-dimensional elements. The numerical model is a FE-based model with 1D and 0D elements. Particular attention is given to the description of the main beams flexural mode shapes. The antenna model, shown in Figure 3 (left), is built by revolving a planar module, shown in Figure 3 (right).

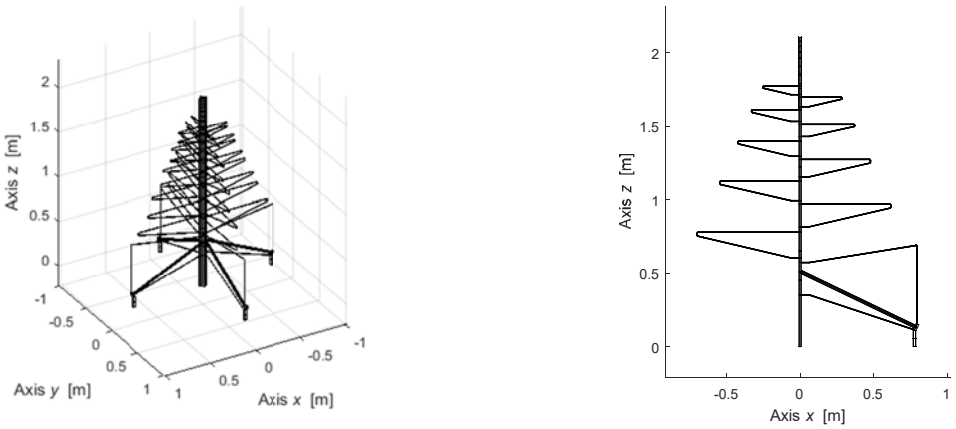

Figure 3: FE model: complete structure (left) and single module (right)

Timoshenko 1D beam elements [16] are used to represent the central main beam, the 9 branches, the 3 supports beams of each module of the structure. Each of these components can be considered as beams. The triangular thin plates in the top part of the antenna are stiffer than branches and they are not structural components, hence they are simplified as localised equivalent added masses in the antenna upper section.

The main beam is considered fixed to the metal grid, to reproduce the boundary conditions in Figure 1 (c), while hinges are placed to the Teflon support supports, to reproduce the rotational degrees of freedom (DOF) compatible with bolt joints of the real Teflon supports in Figure 1 (b). Elastic joints are placed in correspondence of Teflon supports on the main beam Figure 1 (d), with equivalent lumped stiffness of 1000 N/m between the four adjacent main beams. The model possess in total 2600 active DOFs.

3 ANTENNA MODAL ANALYSIS

Modal analysis is performed on the antenna to identify the first global modes of the structure. The identification is performed in the frequency range $0 - 25$ Hz, for both experimentally and on the numerical model. The experimental modal properties of the system, natural frequency $f_{n,r}$, damping ratios ζ_r and mode shapes $\mathbf{\Phi}_r$ are identified from the experimental FRFs using ML-MM algorithm [17]. Natural frequencies and mode shapes are computed from the numerical model, solving the related undamped eigen-problem. The global modes resulting from experimental and numerical modal analysis are reported and compared in Table 1. The first two modes are almost coincident eigenvalues representing the first bending global mode shapes of the antenna, shown in Figure 4. The small differences in experimental frequencies are related to not perfect symmetry of the structure in the two planes. Damping ratios are quite aligned as expected for coincident eigenvalues. The numerical mode shapes are perfectly coincident and aligned with the experimental results. The mode shapes related to experimental modes 3 and 4 and numerical 3-32 do not highlight

any contribution of the main beams of the structure, they are modes of the branches. Experimental modes 5 and 6 are the second global bending mode shapes of the antenna in the two planes, shown in Figure 5, together with the corresponding numerical modes 33-34. Also in this case natural frequencies between experimental and numerical model are quite close and the experimentally identified damping ratios of the modes in the two planes are similar.

Branches modes are found in clusters with multiplicity 4, due to the repetitions of identical components around the main Z axis. A lot of these mode clusters are numerical found, identifying the bending of the different levels of branches. An example is reported in Figure 6, where the four bending of the first levels braches can be observed. These mode shapes cannot be experimentally identified because only the main beam is tested.

Table 1: EMA and FE antenna modes.

Numerical		**Experimental**			**Description**
Mode	f_n [Hz]	Mode	f_n [Hz]	ζ [%]	
1	5.072	1	4.34865	1.76815	1st global bending
2	5.072	2	5.16793	1.77066	
33	23.53	5	23.0727	0.650294	2nd global bending
34	23.53	6	23.9875	0.713329	

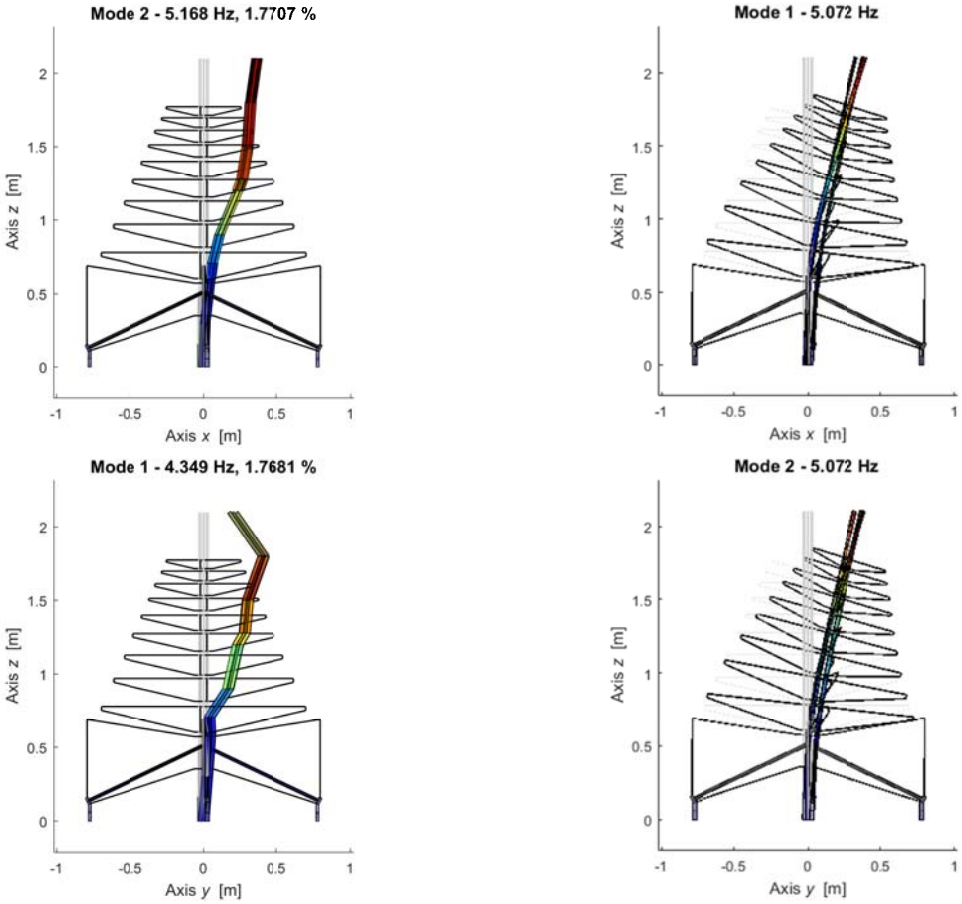

Figure 4: First global bending of the antenna: experimental (left) and numerical (right).

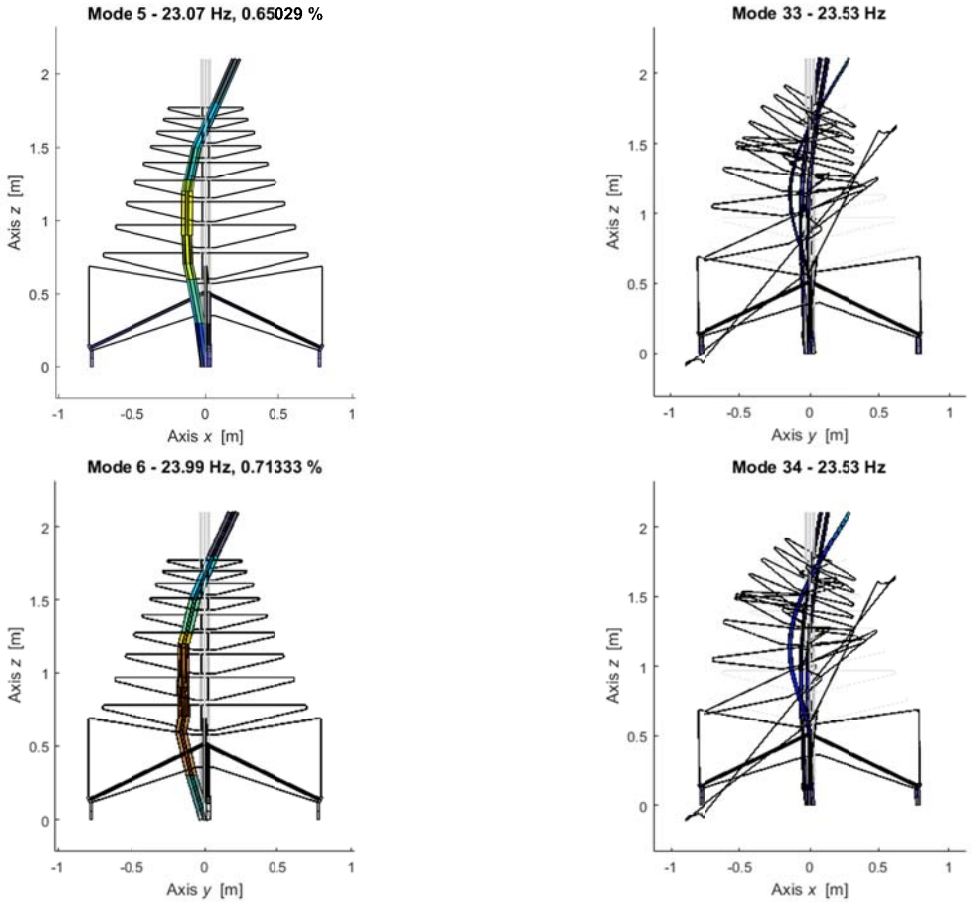

Figure 5: First global bending of the antenna: experimental (left) and numerical (right).

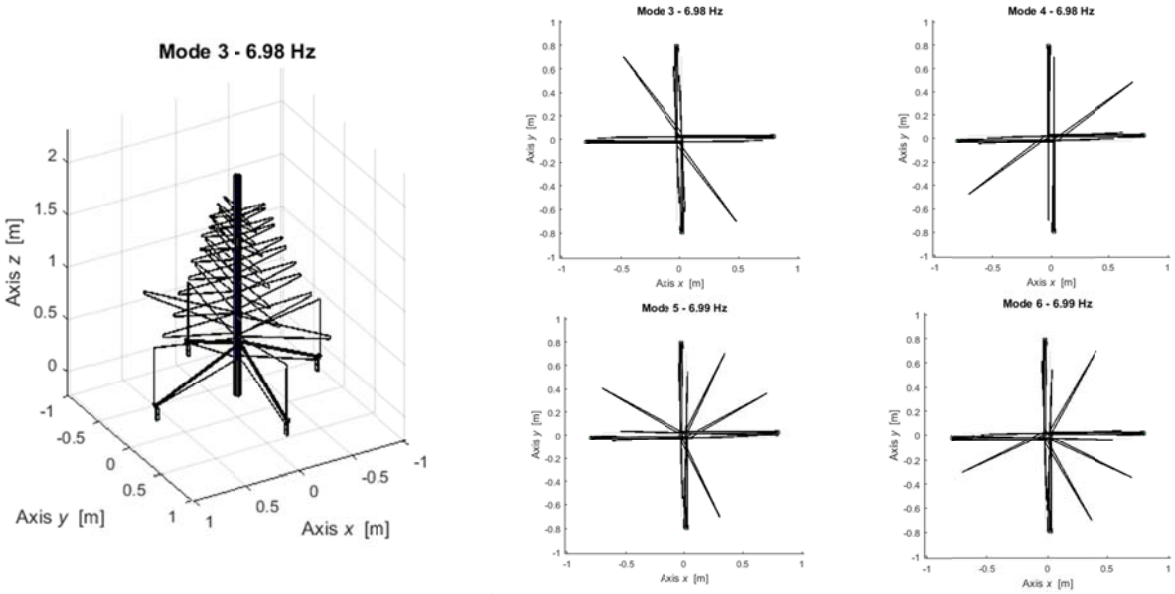

Figure 6: Numerical 1st branches mode shapes in multiplicity four.

4 EXPERIMENTAL EVALUATION OF FLUID-STRUCTURE INTERACTION

The responses of the system during a nonstationary test, with wind speed linearly increases from 13 m/s to 23 m/s, were acquired in the wind tunnel. In particular, the air speed increases into two phases: a first phase from 13 m/s to almost 19 m/s and a second phase from 19 m/s up to 23 m/s. The auto-power spectrograms of the system response in Z direction measured at the lower accelerometer location are shown in Figure 7. The frequencies clearly move with increasing velocity, in different frequency ranges: 40-80, 150-250, 600-1100 Hz. These frequencies are the most representative of aeroelastic effects.

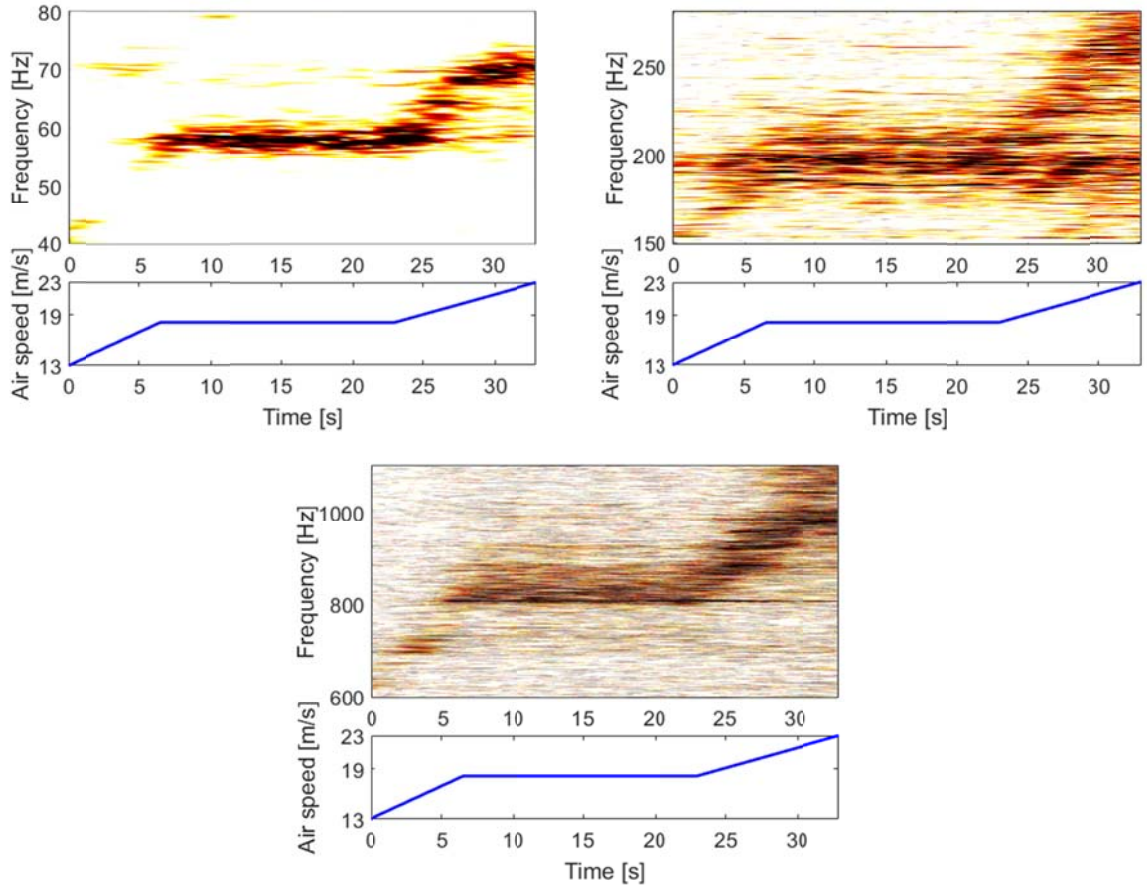

Figure 7: Auto-power spectrograms during air speed transient, measured at $z_1 = 0.65$ m .

The peaks frequencies are more prominent in steady state conditions. Four tests at different constant values of air speed are performed, while acquiring the accelerations of the measured points. The auto-powers of the three stationary signals are computed from the measured responses. The three frequency ranges highlighted before are analysed in Figure 8.

The frequencies associated with the highest energy concentration in the spectrum are clearly visible and are highlighted with vertical dotted lines.

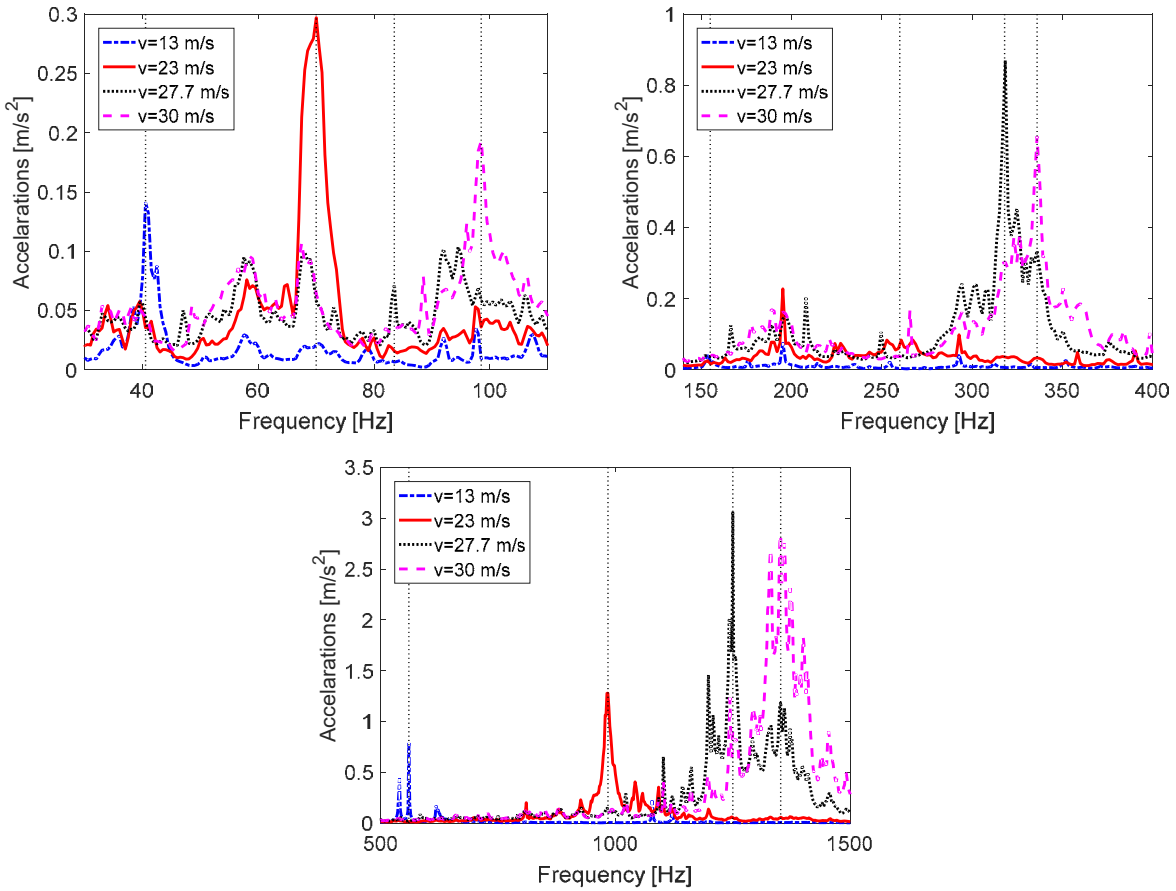

Figure 8: Accelerations Auto-power for different air speed and different ranges of frequencies.

For each wind speed several acceleration peaks emerge whose associated frequencies change according with the speed. Moreover for the three ranges of frequencies the values of the acceleration varies of about one order of magnitude. The highest frequency range involves the highest values of the acceleration, due to the higher wind speed and therefore energy given to the system.

Such frequencies can be linked to the shedding of vortices from the different components of the antenna. It has to be remarked that the antenna under investigation is characterized by different elements with different transversal shapes, lengths, and relative positioning with respect to the wind. Moreover, a very complex interactions between wakes of the components of the antenna takes place, therefore it is not simple to ascribe a specific peak of energy present in the spectrum to a precise component of the antenna from pointwise measurements. From this point of view the identification of the possible responsible is carried out considering that for bluff bodies the Strouhal number, that identifies the non-dimensional frequency associated with the peak of amplitude, is around the value 0.2 for sufficiently high Reynolds number. The Strouhal number is defined as:

$$St = \frac{f_s D}{V} \tag{1}$$

where f_s is the shedding frequency, D is a characteristic dimension of the body and V is the fluid speed. For a circular cylinder D is the diameter of the cross section.

In the present case because of the different shapes of the cross sections, an equivalent reference length has been considered similarly to what is done for the internal flows. We adopted here the concept of hydraulic diameter defined as:

$$D = \frac{4A}{P} \tag{2}$$

where A and P are respectively the area and wetted perimeter of the cross section.

The ratio f_s/V are evaluated for each frequency range from the peak frequencies present in the diagrams of Figure 8. In Table 2 the values of f_s/V are reported. As it can be observed an almost constant value of f_s/V is present varying the air speed in each frequency range.

Table 2: Frequency – air speed ratios.

Velocity V [m/s]	**Ratio** f_s/V [m]		
	Low	**Medium**	**High**
13	3.11	11.92	43.07
23	3.04	11.30	42.78
27.7	3.01	11.48	45.12
33	2.98	10.18	40.96

Assuming that the Strouhal number associated with the shedding phenomenon, as anticipated, is approximately $St \approx 0.2$, it is possible to evaluate the equivalent diameters for the three ranges of frequencies.

$$D_1 = \frac{0.2}{(f_s/V)_1} = 6.58 \text{ cm} \tag{3}$$

$$D_2 = \frac{0.2}{(f_s/V)_2} = 1.78 \text{ cm} \tag{4}$$

$$D_3 = \frac{0.2}{(f_s/V)_3} = 4.7 \text{ mm} \tag{5}$$

The three diameters found can be correlated with the dimensions of the main parts of the antenna. The first characteristic dimension $D_1 = 6.58\,\text{cm}$ is close to the global dimensions of the four beams pack in the antenna centre. The second characteristic dimension $D_2 = 1.78\,\text{cm}$ corresponds to the size of the four supporting bars, and finally the third one $D_3 = 4.7\,\text{mm}$ can be associated to the diameter of the antenna branches. The Reynolds numbers corresponding to the values of these equivalent diameters are in the range $4200 \leq \text{Re} \leq 9700$ for D_1, $16000 \leq \text{Re} \leq 37000$ for D_2, $59000 \leq \text{Re} \leq 136000$ for D_3, sufficiently high to justify the assumption of $S_t = 0.2$.

In Figure 9 two pictures of the antenna for increasing wind speed are reported. As can be

observed the deformed shapes assumed by the antenna are quite close to the first bending mode, due to the transversal load of the tip of the antenna given by the interaction between the triangular surfaces on the tip and the fluid.

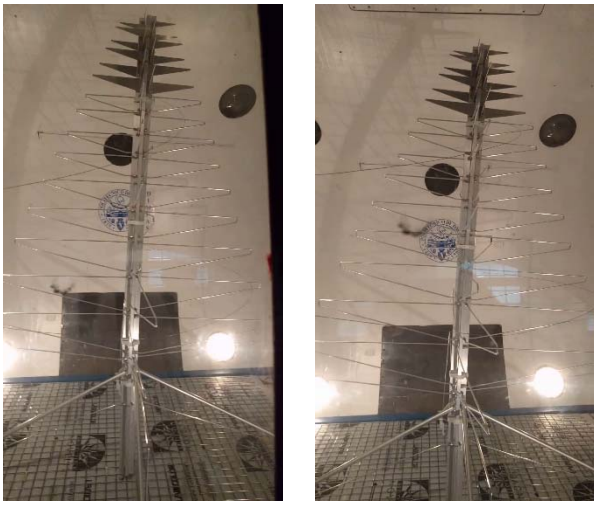

Figure 9: The defection of the antenna at increasing wind speed from left to right. Maximum speed test V =97 km/h.

5 CONCLUSIONS

The dynamics behaviour of an antenna prototype for gravitational waves measurements has been tested in a wind tunnel, to assess its structural deformation under wind load. A numerical model of the structural system is developed, using beam elements and validated. Structural modes of the antenna are experimentally identified in condition of wind off. The antenna presents very high modal density, with several tens of modes within the first 25 Hz. All the modes are computed from the numerical model, while only the global antenna modes are identified from experimental modal analysis. The effects of the fluid structure interaction of the dynamics behaviour of the antenna are studied in a wind tunnel under different air speed condition. Three main frequency range of interaction between the structure and the air flow are evidenced. The effects of shedding phenomena are clearly visible in the identified ranges and the components causing these effects.

Improvements of the antenna can be performed in its structural design to suppress undesirable aeroelastic effects in the low and mid frequency range if they interact with antenna functionality during antenna working conditions.

REFERENCES

[1] www.skatelescope.org, available online in 12/03/2019

[2] de Lera Acedo, E., Razavi-Ghods, N., Troop, N., Drought, N. and Faulkner, A. J. SKALA, a log-periodic array antenna for the SKA-low instrument: design, simulations, tests and system considerations. *Experimental Astronomy* (2015), **39:**567-594**.** DOI: 10.1007/s10686-015-9439-0.

[3] de Lera Acedo E., Drought, N., Wakley, B., Faulkner, A. Evolution of SKALA (SKALA-2), the log-periodic array antenna for the SKA-LOW instrument. *Int. Conf. on Electromagnetics in Adv. Appl.*, Turin, Italy, September 2015.
[4] Di Ninni, P., et al. Mutual Coupling Analysis for a SKA1-LOW Station, *EuCAP 2019*, March 31 – April 5, Krakov, Poland
[5] http://www.sirioantenne.it/it/, available online in 12/03/2019
[6] Virone, G., Lingua, A.M.m Piras, M., Cina, A., Perini, F., Monari, J., Paonessa, F., Peverini, O.A., Addamo, G., Tascone, R. Antenna Pattern Verification System Based on a Micro Unmanned Aerial Vehicle (UAV). *IEEE Antennas and Wireless Propagation Letters* (2014) **13**:169-172. DOI: 10.1109/LAWP.2014.2298250, SKA-BD-28-05
[7] Williamson, C. Oblique and parallel modes of vortex shedding in the wake of a circular cylinder at low Reynolds numbers. *Journal of Fluid Mechanics* (1989) **206**:579-627.
[8] Hu, G., Tse, K.T., Kwok, K.C.S. Aerodynamic mechanisms of galloping of an inclined square cylinder. *J. WindEng.Ind.Aerodyn.* (2016)**148:**6–17.
[9] de Lera Acedo, E., Bolli, p., Paonessa, F., Virone, G., Colin-Beltran, E., Razavi-Ghods, N., Aicardi, I., Lingua, A., Maschio, P., Monari, J., Naldi, G., Piras, G., Pupillo, G. SKA Aperture Array Verification System: Electromagnetic modeling and beam pattern measurements using a micro UAV. *Experimental Astronomy* (2018) **45**(1):1–20. DOI: 10.1007/s10686-017-9566-x
[10] Nguyen, C.H., Freda, A., Solari, G., Tubino, F. Wind–induced instability of complex lighting poles and antennas masts: static and aeroelastic experimental study. *The Eighth Asia-Pacific Conference on Wind Engineering*, December 10–14, 2013, Chennai, India.
[11] Clobes, M., Buffeting Wind Load on Antennas with Rooftop Site. *J. Civil Environ. Eng.* (2015) 5:5.
[12] Maia, M.M.N., Silva, J.M.M. *Theoretical and Experimental Modal Analysis*. Wiley, (1997), New York, USA.
[13] Friswell, M.I., Mottershead, J.E. *Finite Element Model Updating in Structural Dynamics* Dordrecht, Kluwer, 1995.
[14] Bonisoli, E., Brino, M. Robust Updating of Operational Boundary Conditions for a Grinding Machine. Model Validation and Uncertainty Quantification (2015) Springer, Cham, **3**:235-247.
[15] Bonisoli, E., Lupos tutorial, User Manual, Torino, 2018.
[16] Zienkiewicz, O.C., Taylor, R.L., *The finite element method for solid and structural mechanics*, 6th Ed., Elsevier (2005).
[17] El-Kafafy, M., Peeters, B., Guillaume, P., De Troyer, T., Constrained maximum likelihood modal parameter identification applied to structural dynamics. *Mech. Syst. Signal Process*. (2016) **73**:567–589. Doi:10.1016/j.ymssp.2015.10.030.